

# EFFECT OF pH CHANGES ON PHASE CONSTITUENTS, MICROSTRUCTURE AND MAGNETIC PROPERTIES OF NANO-SIZED $\text{NiFe}_2\text{O}_4$ POWDER SYNTHESIZED BY SOL-GEL AUTO-COMBUSTION METHOD

S. Alamolhoda, S. M. Mirkazemi\*, T. Shahjooyi and N. Benvidi

\* [mirkazemi@iust.ac.ir](mailto:mirkazemi@iust.ac.ir)

Received: August 2015

Accepted: January 2016

School of Metallurgy and Materials Engineering, Iran University of Science & Technology, Tehran, Iran.

**Abstract:** Nano-sized  $\text{NiFe}_2\text{O}_4$  powders were synthesized by sol-gel auto-combustion method using pH values from 7 to 9 in the sol. The effect of pH variations on complexing behavior of the species in the sol has been explained. Changes in phase constituents, microstructure and magnetic properties by changes in pH values were evaluated by X-ray diffraction (XRD), field emission scanning electron microscope (FESEM) and vibration sample magnetometer (VSM) techniques. Changes in pH value from 7 to 9 changes the amounts of  $\text{NiFe}_2\text{O}_4$ ,  $\text{FeNi}_3$  and  $\alpha\text{-Fe}_2\text{O}_3$  phases. Calculated mean crystallite sizes are in the range of 44 to 51nm. FESEM micrographs revealed that increasing the pH value to 9 causes formation of coarse particles. Saturation magnetization was increased from 36.96emu/g to 39.35emu/g by increasing pH value from 7 to 8 which is the result of increased  $\text{FeNi}_3$  content. Using higher pH values in the sol reduces the  $M_s$  value.

**Keywords:** Nickel ferrite,  $\text{FeNi}_3$ , pH, Sol-gel auto-combustion, Magnetic properties.

## 1. INTRODUCTION

Chemically synthesized magnetic nanoparticles have drawn much attention due to the unique magnetic properties derived from small particle sizes and uniform size distribution [1].  $\text{NiFe}_2\text{O}_4$  nanoparticles, as one of the most important materials in the inverse spinel family has been widely studied due to its high electro-magnetic performance, excellent chemical stability and mechanical hardness, high coercivity, and moderate saturation magnetization. These properties made it a good contender for the application as soft magnets and low loss materials at high frequencies [2-4]. Nanoparticles of nickel ferrite are also known for their gas and humidity sensing properties [5]; in addition they are an excellent material for ferrofluids making [6], magnetic resonance imaging (MRI) [7], catalysis [8, 9], high-density data storage [10], magnetic refrigeration[11], etc.

Different chemical processes are used for the synthesis of these nanoparticles including co-precipitation [12], hydrothermal process [13], sol-gel [1] and sol-gel auto-combustion method

[14]. Among these methods, sol-gel auto-combustion method is a unique combination of the ignition and the chemical gelation processes which has the advantages of simple preparation, cost-effectiveness and gentle chemistry route resulting in ultra-fine and homogeneous powder [15]. In sol-gel methods complexing process with citric acid is sensitive to pH values [16]. Therefore homogeneity of the sol which is an important parameter for phase formation [17] would be affected by pH of the solution.

Pradeep et. al. had been synthesized nanoparticles of  $\text{NiFe}_2\text{O}_4$  through sol-gel auto combustion method fixing the pH value in the sol equal to 7 and 8 [18]. However they did not studied the effect of pH changes on microstructure and magnetic properties of the synthesized samples.

In this research nano sized powders of nickel ferrite have been synthesized by sol-gel auto-combustion method. The effect of pH variations on complexing behavior of species in the sol, phase formation, microstructure and magnetic properties of the synthesized powders has been studied.

## 2. MATERIALS AND METHODS

Proper amounts of metal nitrates: 7.35 g  $\text{Fe}(\text{NO}_3)_3 \cdot 9\text{H}_2\text{O}$  (99% Merck) and 2.56 g  $\text{Ni}(\text{NO}_3)_2 \cdot 6\text{H}_2\text{O}$  (99% Merck) were dissolved into 50 ml distilled water to make an aqueous solution. The molar ratio of Ni/Fe was fixed to  $\frac{1}{2}$ . Then 5.25 g citric acid ( $\text{C}_6\text{H}_8\text{O}_7$ , 99% Merck) was added to the above mixture as a chelating agent with a nitrate to citrate ratio of 1:1. The solution was heated at  $60^\circ\text{C}$  on magnetic stirrer with a rotating speed of 300rpm to form a clear and green sol with  $\text{pH} < 1$ . The pH value of the solution was raised to 7, 8 and 9 in different samples by addition of ammonia solution. The resulting sol was heated at constant temperature of  $80^\circ\text{C}$  on magnetic stirrer to complete the reaction for forming the gel precursor. Then the gel undergoes a self-ignition reaction to form a very fine brown foamy powder. The samples were coded according to their pH values as p7, p8 and p9 respectively. The phase identification of the combustion products has been performed by

Philips X'pert Pro X-ray diffractometer (XRD) using  $\text{Cu K}\alpha$  radiation ( $\lambda = 0.1541 \text{ nm}$ ). Mean crystallite size of  $\text{NiFe}_2\text{O}_4$  is calculated using Scherrer's equation:

$$D = 0.9 \lambda / \beta \cos\theta \quad (1)$$

where  $D$  is mean crystallite size,  $\lambda$  is the X-ray wavelength,  $\beta$  is the value of the full width at half maximum of the diffraction peaks, and  $\theta$  is the diffraction angle at the peak maxima [19].

XRD patterns were submitted to a quantitative analysis by the Rietveld method using MAUD (material analysis using diffraction) software [20]. The morphology and microstructure of the nano particles were studied by a field emission scanning electron microscope (FESEM) model (TESCAN). Magnetic properties have been taken out at room temperature at the maximum applied field of 14kOe by vibrating sample magnetometer (VSM) model MDK.

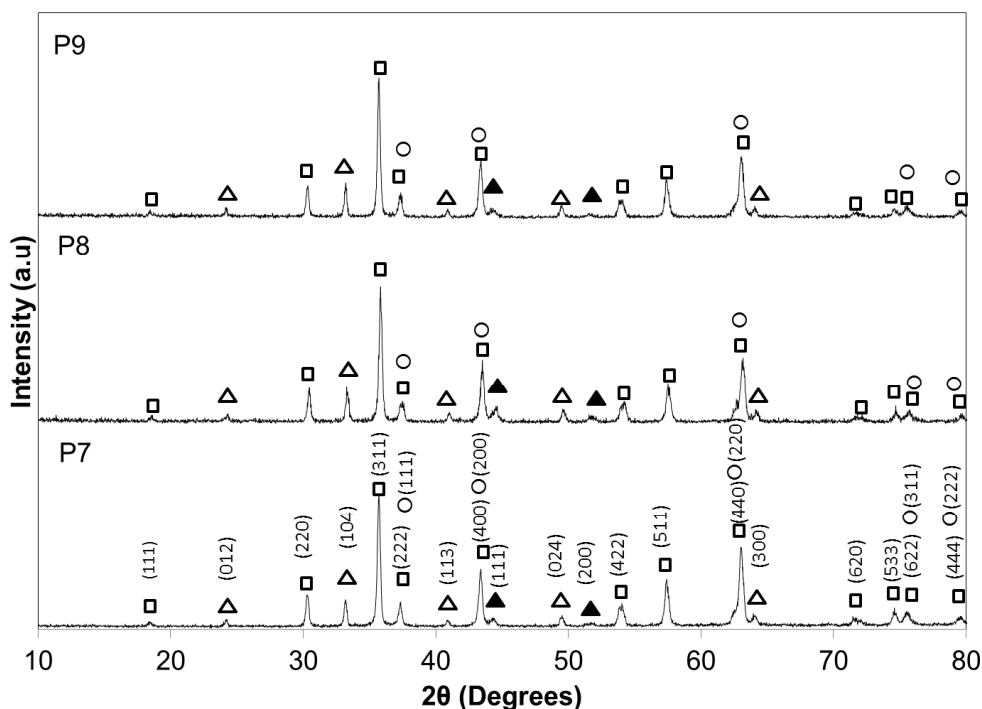


Fig. 1. XRD patterns of the combustion products for samples p7, p8 and p9.  $\square$ :  $\text{NiFe}_2\text{O}_4$ ,  $\Delta$ :  $\alpha\text{-Fe}_2\text{O}_3$ ,  $\blacktriangle$ :  $\text{FeNi}_3$ ,  $\circ$ :  $\text{NiO}$ .

### 3. RESULTS AND DISCUSSIONS

Fig. 1 represents XRD patterns of the combustion products for samples p7, p8 and p9. The combustion product in all of the samples consists of  $\text{NiFe}_2\text{O}_4$ , awaruite ( $\text{FeNi}_3$ ) and hematite phases. Other present reports on the synthesis of  $\text{NiFe}_2\text{O}_4$  by sol-gel auto-combustion method using the same starting materials are in consistent with our results [21, 22]. Formation of  $\text{FeNi}_3$  phase is reported to be as a result of the existence of citric acid since it consumes most of the oxygen surrounding the precursor at the combustion stage. Therefore Fe and Ni metal ions form  $\text{FeNi}_3$  phase as a result of scarcity of oxygen [23].

Peaks of NiO phase in the standard JCPDS 73-1519 are overlapping with  $\text{NiFe}_2\text{O}_4$  peaks in the standard JCPDS 74-2081 card. Therefore presence of NiO phase is probable in the samples. In the standard JCPDS 74-2081 for  $\text{NiFe}_2\text{O}_4$  phase the intensity of (222) and (400) planes reflection at  $37.33^\circ$ ,  $43.375^\circ$  is reported to be equal to 7.4 and 20.2% respectively and in the standard JCPDS 73-1519 for NiO phase the intensity of (111) and (200) planes reflection at  $37.33^\circ$  and  $43.38^\circ$  are equal to 67.7 and 100% respectively. The intensity of (222) and (400) reflections in the XRD pattern of sample P7 are equal to 18.51 and 41.48%. These intensities are

stronger than the observed intensities in the standard JCPDS 74-2081 for  $\text{NiFe}_2\text{O}_4$ . This increased intensity might be as a result of presence of NiO phase. Also in our previous studies Raman spectroscopies proved presence of NiO in the combustion product of a sample prepared in the same condition [24].

The relative intensity of  $2\theta=33.2$  peak ((104) peak of hematite) to  $2\theta=30.3$  peak ((220) peak of ferrite) increased in samples p8, p9. The increment in hematite phase could be studied by the relative concentration of iron and nickel citrates under different pH values in the sol [19, 25] which is represented in Fig. 2. As it could be observed, the ionization of citric acid increases until the pH value reaches to 7. Therefore the more carboxylate groups ( $-\text{COOH}$ ) were formed to chelate  $\text{Fe}^{3+}$  and  $\text{Ni}^{2+}$  ions and hence the formed gel would be more uniform [17, 25]. The relative concentration of the  $\text{Ni}(\text{HCit})$  complexes reaches to a maximum of 40% at pH 3.5 and decreased near to 0 at pH 6 and relative concentration of  $\text{Ni}(\text{Cit})^-$  increases at  $\text{pH}>3.5$  and reaches to maximum concentration of about 100% at pH 7. So nickel can form complex by citrate completely and there is no decrease even if the pH value of the solution approached to 9 [25].  $\text{Fe}(\text{HCit}^+)$  complexes reaches to maximum of 40% at pH 1 and then decrease to zero at pH 4.  $\text{Fe}^{3+}$  would form complexes with citrate at pH 4

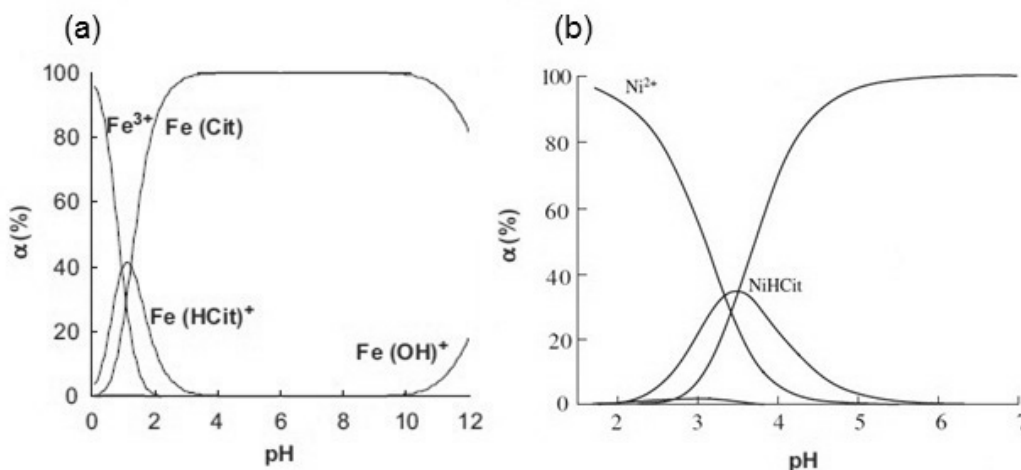


Fig. 2. The yield of the complex species ( $\alpha$ ) vs. pH of the solution for a) Fe ions [19] and b) Ni ions [25].

**Table 1.** Approximated weight percentages of different phases using MAUD software and magnetic properties of the combustion products

Sample Code	NiFe <sub>2</sub> O <sub>4</sub> (wt%)	$\alpha$ -Fe <sub>2</sub> O <sub>3</sub> (wt%)	NiO (wt%)	FeNi <sub>3</sub> (wt%)	Mean crystallite size (nm)
P7	63.65	22.4	12.14	1.78	46
P8	56.31	27.34	13.04	3.31	44
P9	60.29	23.79	13.76	2.15	51

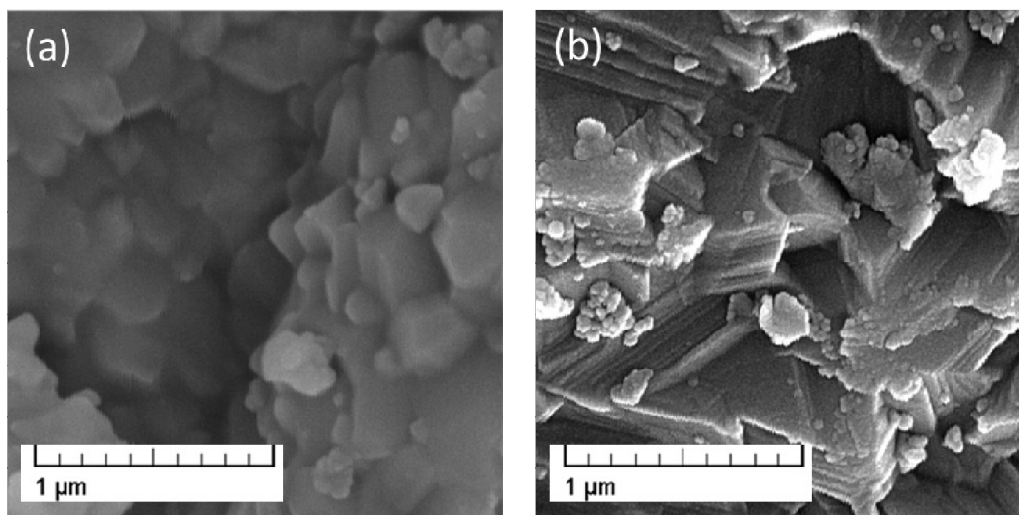
and higher in the form of FeCit. The graph represents that at pH values around 10, Fe ions precipitate as hydroxide which lowers the amount of formed complexes in the sol.

In addition to above mentioned phases, presence of NiO phase is also probable since all of NiO XRD peaks overlap with NiFe<sub>2</sub>O<sub>4</sub> peaks. Quantitative analyses performed by Rietveld method using MAUD software are shown in table 1. It should be noted that these quantities are just rough approximations and they are not exact; however they can represent relative phase changes by changes in pH content.

The approximated phase quantities represent that when pH value reaches to 8, hematite phase content increases about 5%, this may be as a result of precipitation of iron hydroxide in the sol, which forms hematite phase in the combustion product. As a result of precipitation

of iron hydroxide in the sol the chelation of metal ions with citrates would be poor. This leads to incomplete 3D net-structured gel. Therefore the oxidants in the gel would be easily decomposed before the combustion process [26]. Therefore the combustion atmosphere would be more reductive and higher amount of FeNi<sub>3</sub> would be formed.

Table 1 represents that when the pH value reaches to 9, the amount of hematite and FeNi<sub>3</sub> phases again decreases and reaches to amounts near the ones obtained for sample P7. It seems that because of the higher amount of NH<sub>4</sub>NO<sub>3</sub> formation in this sample, the amount of released heat would be increased [18]. The higher released heat could increase the combustion temperature and therefore could provide proper conditions for oxidation of FeNi<sub>3</sub> phase. Therefore less amount of FeNi<sub>3</sub> and higher amount of  $\alpha$ -Fe<sub>2</sub>O<sub>3</sub> could be

**Fig. 3.** FESEM images of the samples a) P7 and b) P9.

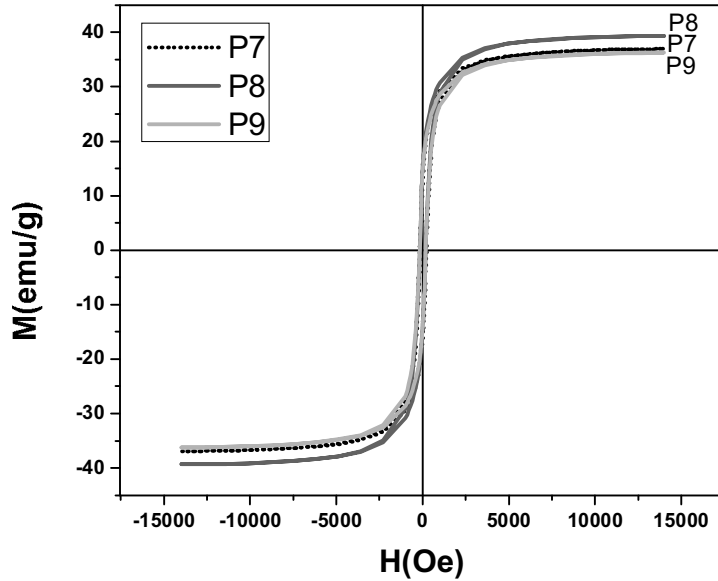


Fig. 4. VSM plots of P7, P8 and P9 samples.

observed in this sample. Also the higher obtained temperatures could result in formation of higher amounts of  $\text{NiFe}_2\text{O}_4$ . The calculated values for mean crystallite sizes of the samples are shown in table 1. As it could be observed the mean crystallite sizes of the samples are in the range of 44 to 51 nm.

FESEM images of the samples P7, P9 are shown in Fig. 3. The images show that the morphology and size of the particles in the combustion products would be affected by pH value of the sol. The higher released heat in the redox reaction of the gel as a result of presence of higher amount of  $\text{NH}_4\text{NO}_3$  might be the reason of formation of coarse particles with higher crystallinity as the pH value of the sol reaches to 9.

Table 2. Magnetic properties of the synthesized samples

Sample Code	$M_s$ (emu/g)	$iH_c$ (Oe)	$M_r$ (emu/g)
P7	36.9	175.5	14.6
P8	39.3	178.6	14.9
P9	36.2	180.6	14.3

Magnetization curves of the samples obtained from room temperature VSM measurements are shown in Fig. 4.  $M_s$ ,  $M_r$  and  $iH_c$  quantities of the samples are listed in table 2. The results show that changes in pH value affects  $M_s$  values. There is a relationship between the calculated  $M_s$  values and phase constituents of the samples. As it could be observed, the highest  $M_s$  value is obtained in sample P8 which has the highest amount of  $\text{FeNi}_3$  phase. The reported saturation magnetization for bulk sample of single phase  $\text{NiFe}_2\text{O}_4$  is equal to 55 emu/g [27] while the reported values for its nanoparticles are 50.4 [14] and 46.53 emu/g [11] and the reported value for  $\text{FeNi}_3$  is equal to 110 emu/g [28]. It could be observed that the highest value of  $M_s$  is obtained in sample P8 which has the lowest amount of  $\text{NiFe}_2\text{O}_4$  which is about 56 wt. % and highest amount of  $\text{FeNi}_3$  which is about 3 wt. %. The  $M_s$  value of the two other samples are nearly the same since the amount of  $\text{FeNi}_3$  and  $\text{NiFe}_2\text{O}_4$  in these samples are near to each other.

#### 4. CONCLUSIONS

Nano-sized  $\text{NiFe}_2\text{O}_4$  powders were synthesized by sol-gel auto-combustion method using pH values of 7, 8 and 9 in the sol. The

results represents that the combustion product consists of  $\text{NiFe}_2\text{O}_4$  as the main phase and some amounts of  $\alpha\text{-Fe}_2\text{O}_3$ ,  $\text{FeNi}_3$  and  $\text{NiO}$ .  $M_s$  values of the samples are influenced by pH changes since the amount of obtained phases are influenced by pH variations. FESEM results reveals that increasing the pH value to 9 causes formation of coarse particles with higher crystallinity. Magnetic measurements showed that the highest amount of  $M_s$  which was equal to 39.3 emu/g was obtained in the sample synthesized with pH value of 8 since there is higher amount of  $\text{FeNi}_3$  phase in that sample. Changing pH value to 7 or 9 decreases the  $M_s$  values since the amount of formed  $\text{FeNi}_3$  phase would be decreased.

## REFERENCES

1. Liu, X., Fu, S. and Huang, C., "Magnetic properties of Ni ferrite nanocrystals dispersed in the silica matrix by sol-gel technique". *J. Magn. Magn. Mater.*, 2004, 281, 234-239.
2. Wang, H., Zhang, F., Zhang, W., Wang, X., Lu, Z., Qian, Z., Sui, Y., Dong, D. and Su, W., "The effect of surface modification on the morphology and magnetic properties of  $\text{NiFe}_2\text{O}_4$  nanoparticles". *J. Cryst. Growth*, 2006, 293, 169-174.
3. Khairy, M., "Synthesis, characterization, magnetic and electrical properties of polyaniline /  $\text{NiFe}_2\text{O}_4$  nanocomposite". *Synthetic Met.*, 2014, 189, 34-41.
4. Prabhakaran, T. and Hemalatha, J., "Combustion synthesis and characterization of highly crystalline single phase nickel ferrite nanoparticles". *J. Alloys Compd.*, 2011, 509, 7071-7077.
5. Satyanarayana, L., Reddy, K. M. and Manorama, S. V., "Nanosized spinel  $\text{NiFe}_2\text{O}_4$ : A novel material for the detection of liquefied petroleum gas in air". *Mater. Chem. Phys.*, 2003, 82, 21-26.
6. Raj, K., Moskowitz, B. and Casciari, R., "Advances in ferrofluid technology". *J. Magn. Magn. Mater.*, 1995, 149, 174-180.
7. Manuel Perez, J., Joseph Simeone, F., Tsourkas, A., Josephson, L., and Weissleder, R., "Peroxidase substrate nanosensors for MR imaging". *Nano letters*, 2004, 4, 119-122.
8. Rashad, M. M. and Fouad, O. A., "Synthesis and characterization of nano-sized nickel ferrites from fly ash for catalytic oxidation of CO". *Mater. Chem. Phys.*, 2005, 94, 365-370.
9. Ma, L. J., Chen, L. S. and Chen, S. Y., "Study of the  $\text{CO}_2$  decomposition over doped Ni-ferrites". *J. Phys. Chem. Solids*, 2007, 68, 1330-1335.
10. Speliotis, D. E., "Magnetic recording beyond the first 100 years". *J. Magn. Magn. Mater.* 1999, 193, 29-35.
11. Sivakumar, P., Ramesh, R., Ramanand, A., Ponnusamy, S. and Muthamizhchelvan, C., "Structural, thermal, dielectric and magnetic properties of  $\text{NiFe}_2\text{O}_4$  nanoleaf", *J. Alloys Compd.*, 2012, 537, 203-207.
12. Maaz, K., Karim, S., Mumtaz, A., Hasanain, S. K., Liu, J. and Duan, J. L., "Synthesis and magnetic characterization of nickel ferrite nanoparticles prepared by co-precipitation route". *J. Magn. Magn. Mater.*, 2009, 321, 1838-1842.
13. Komarneni, S., D'Arrigo, M. C., Leonelli, C., Pellacani, G. C. and Katsuki, H., "Microwave-hydrothermal synthesis of nanophase ferrites". *J. Am. Ceram. Soc.*, 1998, 81, 3041-3043.
14. Sivakumar, P., Ramesh, R., Ramanand, A., Ponnusamy, S. and Muthamizhchelvan, C., "Preparation and properties of nickel ferrite ( $\text{NiFe}_2\text{O}_4$ ) nanoparticles via sol-gel auto-combustion method". *Mater. Res. Bull.*, 2011, 46, 2204-2207.
15. Sivakumar, P., Ramesh, R., Ramanand, A., Ponnusamy, S. and Muthamizhchelvan, C., "A simple wet chemical route to synthesize ferromagnetic nickel ferrite nanoparticles in the presence of oleic acid as a surfactant". *J. Mater. Sci.: Mater. Electron.*, 2012, 23, 1041-1044.
16. Zhou, W., Shao, Z. and Jin, W., "Synthesis of nano-crystalline conducting composite oxides based on a non-ion selective combined complexing process for functional applications". *J. Alloys Compd.*, 2006, 426, 368-374.
17. Masoudpanah, S. M. and Seyyed Ebrahimi, S. A., "Effect of pH value on the structural and magnetic properties of nanocrystalline strontium hexaferrite thin films". *J. Magn. Magn. Mater.*, 2011, 323, 2643-2647.
18. Pradeep, A., Priyadharsini, P. and Chandrasekaran, G., "Production of single

- phase nano size  $\text{NiFe}_2\text{O}_4$  particles using sol-gel auto combustion route by optimizing the preparation conditions”. *Mater. Chem. Phys.*, 2008, 112, 572-576.
19. D. Cullity, *Elements of X-ray Diffraction*, 2nd edn, Addison-Wesley, London, 1987, p.102.
  20. Rietveld, H. M., “A profile refinement method for nuclear and magnetic structures”. *J. Appl. Cryst.*, 1969, 2, 65-71.
  21. Azadmanjiri, J. and Seyyed Ebrahimi, S. A., “The effects of pH and citric acid concentration on the characteristics of nano-crystalline  $\text{NiFe}_2\text{O}_4$  powder synthesized by a sol-gel auto-combustion method”. *Phys. Met. Metallogr.*, 2006, 102, S21-S23.
  22. Azadmanjiri, J., Seyyed Ebrahimi, S. A. and Salehani, H. K., “Magnetic properties of nanosize  $\text{NiFe}_2\text{O}_4$  particles synthesized by sol-gel auto combustion method”. *Ceram. Int.*, 2007, 33, 1623-1625.
  23. Zhu, J., Xiao, D., Li, J., Yang, X. and Wu, Y., “Characterization of  $\text{FeNi}_3$  alloy in Fe-Ni-O system synthesized by citric acid combustion method”. *Scripta Mater.*, 2006, 54, 109-113.
  24. Alamolhoda, S., Mirkazemi, S. M., Benvidi, N., Shahjooyi, T., “Effect of fuel-to-oxidant ratio on phase constituents, microstructure and magnetic properties of  $\text{NiFe}_2\text{O}_4$  based composite nanopowder synthesized by sol-gel auto-combustion method”. *J. Sol-Gel Sci. Technol.*, Article in press, DOI 10.1007/s10971-015-3880-4.
  25. Zelenin, O. Yu., “Interaction of the  $\text{Ni}^{2+}$  ion with citric acid in an aqueous solution”, *Russ. J. Coord. Chem.*, 2007, 33, 346-350.
  26. Ge, L., Zhou, W., Ran, R., Shao, Z., Liu, S., “Facile auto combustion synthesis of  $\text{La}_{0.6}\text{Sr}_{0.4}\text{Co}_{0.2}\text{Fe}_{0.8}\text{O}_3$ -d (LSCF) perovskite via a modified complexing sol-gel process with  $\text{NH}_4\text{NO}_3$  as combustion aid”. *J. Alloys Compd.*, 2008, 450,338-347.
  27. Mulson, A. J. and Herbert, G. M., “*Electroceramics, Materials, Properties, Applications*”, 2nd edn, Wiley & Sons Inc, London, 2003.
  28. Lu, X., Liang, G. and Zhang, Y., “Synthesis and characterization of magnetic  $\text{FeNi}_3$  particles obtained by hydrazine reduction in aqueous solution”. *Mater. Sci. Eng. B*, 2007, 139,124-127.